CIRP Annals - Manufacturing Technology 62 (2013) 295–298

Contents lists available at SciVerse ScienceDirect

CIRP Annals - Manufacturing Technology

journal homepage: http://ees.elsevier.com/cirp/default.asp

On the linear friction welding process of aluminum alloys: Experimental insights through process monitoring

Livan Fratini (2)*, Gianluca Buffa, Marco Cammalleri, Davide Campanella

Department of Chemical, Management, Computer Science, Mechanical Engineering, University of Palermo, Viale delle Scienze, 90128 Palermo, Italy

ARTICLE INFO

Keywords:
Joining
Aluminum
Linear Friction Welding

ABSTRACT

Linear friction welding is a solid-state joining process for non-axisymmetric components in which joining of materials is obtained through the relative motion of two components under pressure. In the process the heat source is given by the frictional forces work decaying into heat determining a local softening of the material and eventually bonding conditions. A dedicated fixture was equipped with sensors for the in-process acquisition of variables regarding kinematics, dynamics and temperature levels. The results of an experimental campaign aimed to weld AA6082-T6 aluminum alloy parts are presented and a process window is identified for the used alloy.

1. Introduction

Solid state bonding phenomena occur in several processes of different nature as Porthole Die Extrusion [1], Accumulative Roll Bonding (ARB) [2] and friction welding operations. Among the latter, three different operations can be identified: Friction Stir Welding (FSW), the most recently introduced one, in which the stirring action of a tool with a pin at its end activates a material flow allowing to join blanks of several "difficult to be welded" light alloys as aluminum alloys [3] and titanium alloys [4]; Rotary Friction Welding (RFW) and Inertia Friction Welding (IFW) [5], used to join axisymmetric parts with particular reference to tubes; Linear Friction Welding (LFW), used to join non-axisymmetric thick parts. The latter is the eldest among the friction welding processes, being first patented in 1929. However the process has never been actually used to produce parts up to a few years ago because of technical limitations in building proper machines. In the process the two parts to be welded are put in a reciprocating motion, with large oscillation frequency, under a certain pressure. The heat generated by the friction forces work softens the material and eventually allows to get solid bonding conditions [6]. Vairis and Frost were the first to identify and describe the main phases of the process. In particular, during the initial phase, the reciprocating motion begins and the actual contact surface is less than 100% of the transverse sections of the specimens. If proper combination of the process parameters is selected, sufficient heat is generated and the transition phase is reached. During this phase the actual contact surface is 100% of the specimens transverse section and plastic deformation of material at the interface begins due to the reached softening state. Then, the equilibrium phase starts as the softened material is extruded under the applied pressure. Finally, during the deceleration phase, the reciprocating motion is stopped and additional pressure can be applied for a few seconds on the specimens in order to consolidate the weld. From the given short description, it arises that the process is characterized by a number of advantages over traditional welding processes. First, as a solid state process, it permits welding of materials considered "not weldable" or difficult to be welded by traditional fusion welding processes. Additionally inclusions, porosities, formation of brittle phases and solidification cracks are avoided and no fumes or sparks are generated. Then, the weld is very quick as sound parts can be obtained in a few seconds even on thick specimens. Finally, no specific part preparation is required and oxidation is reduced because oxides are expelled from the interface together with the flash during the equilibrium phase. On the other hand, one of the main drawbacks is the elevated cost of the LFW machine, which has to provide large oscillation frequencies and extreme stiffness [7]. For this reason at the beginning the process has been used only for high added value products as the aeroengine blisks, i.e. the bladed disks of aeroengine compressors [8]. The commonly used materials are titanium [6] and nickel alloys [9]. Both these materials show an extremely low thermal conductivity, so they are suited for the process as retain the heat close to the interface, namely where the heat is generated. However, interesting studies can be found on other materials as steels [10], tungsten and cobalt alloys [7].

As far as aluminum alloys are regarded, only very few studies can be found in literature, and just one is focused on non-MMC joints [11]. In the paper the authors focus on the microstructural and mechanical characterization of AA2024 joints, both from the static and the dynamic point of view, using just one set of process parameters for the experiments. It is worthy notice that LFW of aluminum alloys presents additional difficulties due to the large thermal conductivity of these materials. In this way large values of frequency and pressure, with respect to the material flow stress at the processing temperatures, are needed and the process parameters window for sound joints is reduced. On the basis of the results that the cited researches found for LFW of materials other than titanium and nickel alloys, it arises that the potential of the

* Corresponding author.

0007-8506/$ – see front matter © 2013 CIRP.
http://dx.doi.org/10.1016/j.cirp.2013.03.056

process is much wider than what explored so far. The lack of knowledge present in the state of the art is due to the difficulty to carry out an effective tuning of the process because of the material thermo-mechanical characteristics.

In order to face the latter issue, in the paper an experimental campaign is developed on LFW of AA6082-T6 aluminum alloy for structural applications on thick parts not weldable by FSW. Although weldable by traditional fusion welding techniques, this material shows very poor resistance in the welded area. Structural applications require more performing joints and solid state processes can represent an effective solution. In order to develop the experimental campaign, a previously in-house designed and built LFW machine was equipped with measuring sensors. A process parameters window for the utilized alloy was identified and the effects of the analyzed process variables were highlighted.

2. Experimental tests

2.1. LFW machine

The machine used for the experiments was characterized by a desmodromic kinematic chain [12] used to obtain the oscillation motion of the bottom specimen. In order to widen the available range of oscillation frequency, interchangeable three lobes cams were used. It should be observed that in previous application on steel specimens dual-lobe cams were used. As a matter of fact, aluminum alloys show higher thermal conductivity with respect to steel and maintaining the same range of pressure values on the specimens, larger oscillation frequency values must be reached in order to obtain sound joints. Proper pressure was applied on the top specimen via a double-acting hydraulic actuator, mounted on a steel rack and controlled by an electro-valve, allowing loads up to 15,000 KN. The already developed machine capabilities were enhanced with the introduction of a number of devices and sensors controlled by a unique interface. In order to stop the reciprocating motion at the pre-determined process time and to reduce the machine inertia to obtain a quick stop, a pneumatic clutch was positioned on a secondary shaft and connected to the cam one. Finally, on the secondary shaft a speed-torque meter and a fly wheel were mounted to measure the required power. Fig. 1 shows a sketch of the main components of the machine.

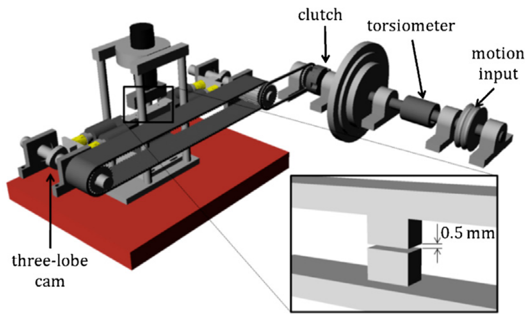

Fig. 1. Sketch of the machine with specimens at the starting position.

The driver speed and torque were measured by a Tekkal TT-4000 speed-torque meter of the strain-gauge type, while the motion of the mobile specimen was measured by a Bruel&Kjaer 4371 accelerometer of piezoelectric type and Bruel&Kjaer 2626 charge amplifier. The temperature of the specimen was picked up by a thermocouple of K-type. The clutch was controlled by a pneumatic SMC solenoid valve. All signals were conveyed to a National Instruments DAQ Card 6062 12 bit 500 kSa/s by means of a BNC-2120 connector accessory and analyzed by a proper routine programmed with LabVIEW. In this way a unique panel was used to control the machine and monitor the process variables during and after the developed tests.

2.2. Developed tests

The as received AA6082-T6 bars were reduced in specimen characterized by height of 10 mm and cross-sectional dimensions at the contact interface equal to 10 mm $\times$ 7 mm. A hole 1 mm in diameter was drilled on the lateral surface of the top specimen at a distance of 6 mm from the interface surface in order to place a K-type thermocouple for temperature acquisition during the process. High conductivity glue was used to obtain a stable contact between the thermocouple and the specimen.

Variable oscillation frequency and applied pressure were used during the tests, while constant oscillation amplitude and process time were selected. In particular the latter parameter was set on the basis of the results of a preliminary experimental campaign. For each test the starting condition corresponded to a distance of the two contact surfaces equal to 0.5 mm. Once the oscillation reached the steady state the oleo-dynamic actuator valve was opened via software and pressure was applied. The contact between the two specimens was considered as starting time for the temporized pneumatic clutch. In this way the burn-off time was utilized for tests control and stop. During the deceleration phase an additional pressure, equal to 20% of the test pressure, was given to the joint for 5 s. Each test was repeated three times and excellent repeatability was found in terms of sound/poor weld obtainment. Table 1 shows the used process parameters. Transverse sections were cut from each joint. The specimens were hot mounted, polished and etched with Keller reagent.

Table 1
Process variables values used for the experiments.

Process variable	Value(s)
Frequency f [Hz]	36, 45, 58
Pressure p [MPa]	20, 30, 40, 50, 60
Amplitude A [mm]	2
Time t [s]	1.25

3. Results

First of all a process map was built. Three different conditions were identified from the analysis of the welded joints: “sound” joints were defined those for which an actual bond was obtained with the full development of the different stages of the process mechanics. As the selected process parameters resulted in failure to pass the initial or the transition process phase into the equilibrium one, the joints were labeled as “insufficient heat”. In these cases no actual bonding is observed and the two specimens are separated at the end of the process. Finally, as large pressure and frequency values were selected, the excess of heat caused an uncontrollable burn-off leading to the collapse of the specimens. These conditions were labeled as “instability”.

In order to build the process map a summarizing parameter W was used, taking into account the concurrent effect of root mean square amplitude $A/\sqrt{2}$, angular frequency $2\pi f$ and pressure p:

$$W = \frac{2\pi f A p}{\sqrt{2}} \quad [\mathrm{kW/mm^2}] \qquad (1)$$

where A is expressed in mm, f in Hz and p in Mpa. According to the used units the parameter W conventionally represents the power per surface unit conferred to the joints. This parameter was derived from the one proposed in [6]. In Fig. 2 the obtained process map is shown at the varying of W as function of the oscillation frequency [6]. In the figure a process window is identified: for low oscillation frequencies, no sound weld can be obtained regardless of the utilized W, i.e. of the applied pressure since the amplitude of oscillation was kept constant (Table 1). At the increasing of the oscillation frequency, namely at 45 Hz and 58 Hz, sound joints can be obtained. For both frequency levels, as low specific power is

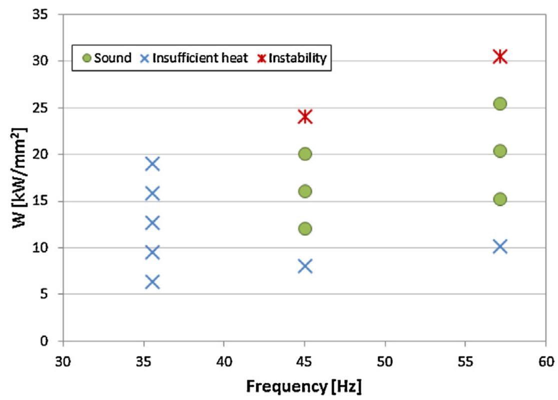

Fig. 2. Process map in the W parameter vs. oscillation frequency plane.

conferred, no weld is obtained; on the contrary, as the conferred power is too large, the instability phenomenon is observed resulting in test failure. Frequency values larger than 58 Hz were not investigated as they exceed the limits of the fixture.

Fig. 3 shows four typical conditions observed during the experimental campaign. In particular, in Fig. 3a a sound weld is shown, obtained with frequency equal to 58 Hz and pressure equal to 40 MPa, resulting in specific power W equal to 20.28 kW/mm^2. The typical flash is visible in both longitudinal and transverse direction indicating that the process correctly reached the equilibrium phase and proper burn-off occurred. Fig. 3b shows the joint obtained with frequency equal to 45 Hz and pressure equal to 30 MPa, resulting in specific power W equal to 12 kW/mm^2. It is worthy notice that this represents a limit condition as a bond is obtained, but the formed flash is poor, indicating that the equilibrium stage has been reached for a limited amount of time during the process. As a matter of fact, a further decrease in the pressure applied at the interface results in no weld for insufficient heat.

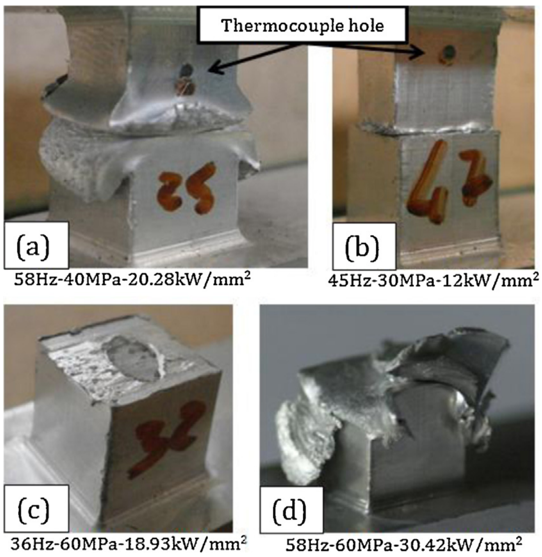

Fig. 3. Typical conditions observed during the experiments: (a) sound joint, (b) bonding limit condition, (c) insufficient heat and (d) instability.

On the other hand, in Fig. 3c a specimen obtained with frequency equal to 36 Hz and pressure equal to 60 MPa, resulting in specific power W equal to 18.93 kW/mm^2, is shown. As it can be seen this conditions represents the typical insufficient heat case study. Because of the applied pressure, and of the consequently reached W value, the bonding process is about to start at the core of the interface between the two specimens. However, the two specimens are easily separable at the end of the process as the equilibrium stage was not reached. Finally, in Fig. 3d a typical instability case study is shown, corresponding to frequency of 58 Hz, pressure 60 MPa and specific power W 30.42 kW/mm^2. In this case the excess of heat conferred to the joint resulted in an instable and uncontrollable burn-off, with a huge amount of flash produced and the top specimen that totally collapsed on the bottom one.

As described in the previous paragraph, temperature was acquired during each test through a thermocouple positioned at a distance of 6 mm from the initial interface between the specimens (see again Fig. 3a and b). In Fig. 4 the obtained curves are shown for selected tests. For the sake of simplicity, each test was labeled with three numbers representing the used frequency and pressure and the resulting W, respectively.

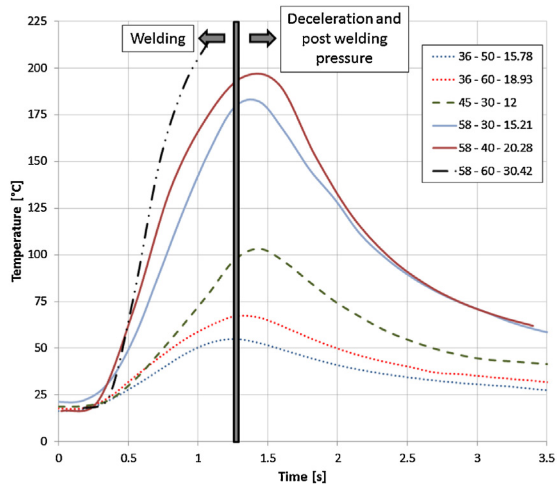

Fig. 4. Temperature vs. time curves for different process conditions.

A few observations can be made from Fig. 4. First, the maximum temperature level is reached, for all the specimens, after the interruption of the reciprocating motion, when the additional pressure is applied. This is due to the fact the temperature is not measured at the interface but at an initial distance from it that varies during the test and between each test, depending on the amount of burn-off occurring due to the selected process parameters. Then, in spite of the elevated frequencies used in this study, larger than the ones typically used for titanium alloys and steels, low temperatures levels are observed. This is due to the high thermal conductivity of aluminum alloys, and represents a difficulty to be overcome in LFW of these alloys. Looking at the 45-30-12 case study, representing the lower bound of the "sound" group, a maximum temperature of about 100 °C was measured. The material is then not sufficiently softened to create a proper flash although a solid bonding is obtained. On the other hand, a further increase in the oscillation frequency leads to larger temperature values, ranging between about 180 °C and 200 °C, and perfect flash conditions. Finally, as the pressure is further increased, a larger heat flux is produced determining instability conditions. The curve corresponding to 58-60-30.42 process conditions is steeper with respect to all the others. However, the high temperature level results in a too softened material that is no more able to carry the applied pressure and collapses, destroying the thermocouple.

The torque required by the machine was acquired during the tests by the torsiometer (Fig. 5). As the two specimens come in contact, the torque rapidly increases till it reaches a steady state after about 0.25 s. As for the temperature levels, lower values, equal to about 22 Nm, are observed for the tests characterized by insufficient heat. Larger torque values are observed for the sound joints, with a significant difference between the lower bound condition, i.e. the 45-30-12 case study, and the others characterized by proper flash, for which a torque in the range of 30–35 Nm is measured. An important difference, with respect to what was found for the temperature levels, is observed for the unstable weld. In this case the torque increases to a steady state value of about

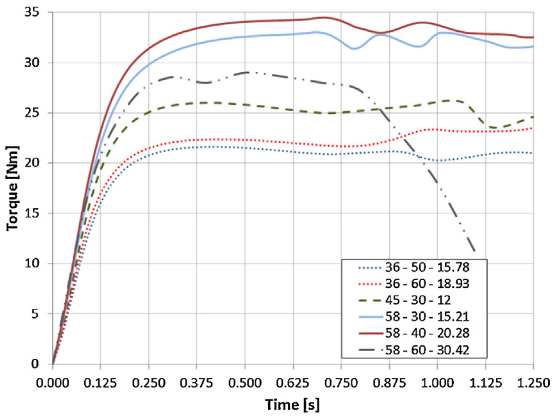

Fig. 5. Torque values vs. time curves for different process conditions.

28 Nm, which is within the range of sound welds, but lower than what measured for welds obtained with same frequency and lower pressure. However, temperature increases rapidly during the unstable test, thus enhancing material softening till the specimens collapse, resulting in a dramatic decrease of the required torque before the fixed process time was reached.

Microhardness measurements were performed on the symmetry plane in the transverse sections of sound welds. Fig. 6 shows the obtained curves for the welded case studies shown in Figs. 4 and 5.

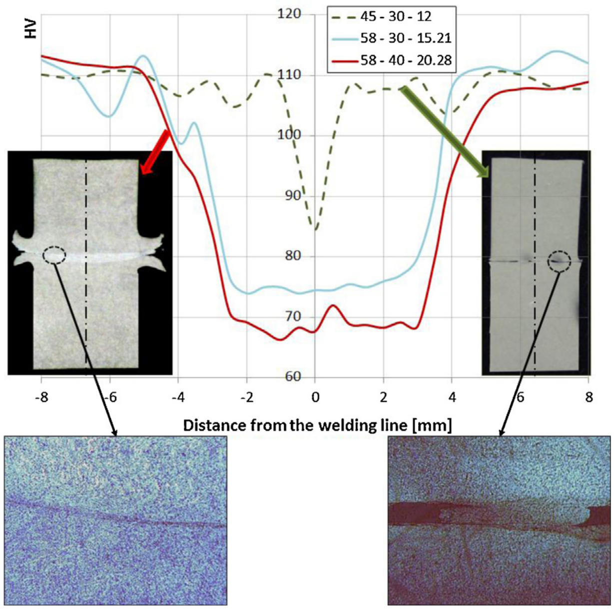

Fig. 6. Microhardness values vs. distance from the welding line for different process conditions.

As expected, a decrease in the microhardness values is observed in the welded zone with respect to the parent material (HV = 110), due to the dissolution of the precipitates occurring in the used precipitation hardened alloy because of the heat flux generated during the process. At the increasing of the heat conferred to the joint both the increase of the softened area extension and the decrease of the HV value at the welding line are observed. For the 45-30-12 weld just a very thin layer close to the welding line is characterized by reduced hardness. However the macro image of the etched transverse section clearly shows an intermittent bonding for the 45-30-12 case study (see dotted circles in Fig. 6), with just small signs of flash, as compared to the same image referred to the 58-40-20.28 case study.

4. Conclusions

In the paper the results of an experimental campaign on LFW of AA6082-T6 aluminum alloy are reported. A dedicated machine was equipped with proper sensors and with a computer controlled pneumatic clutch in order to control the experiment duration. Several tests were performed at the varying of oscillation frequency and pressure at the interface. From the obtained results the following conclusions can be drawn:

- A process window has been identified taking into account the power per surface unit W; because of the extremely high thermal conductivity of aluminum alloys, large frequency values must be used in order to confer proper heat to the weld. What is more, the process window is narrow: for a fixed oscillation frequency value, a wrong choice of the applied pressure can result in either insufficient heat or instability.
- As the reached temperature in the specimen is below a threshold, no solid bonding phenomena are observed. On the other hand, instability conditions are characterized by a rapid increase in temperature till values larger than the ones measured for sound joints, leading to specimens collapse.
- A similar behavior is found for the torque, which must exceed lower bound value in order to produce sound welds. As parameters resulting in joint instability are selected, a steady state torque value within the sound joints range is measured before exaggerate burn-off leads to early failure of the experiment and rapid decrease of the required torque.
- Microhardness decreases in the weld zone due to precipitates dissolution in the utilized AA6082-T6 alloy during welding.

It can be finally stated that the insights of the present research provided new pieces of knowledge to the current state of the art in LFW, assessing the feasibility of the process to AA6082-T6 and identifying a process window for the production of sound joints.

References

[1] Bariani PF, Bruschi S, Ghiotti A (2006) Physical simulation of longitudinal welding in porthole-die extrusion. *CIRP Annals – Manufacturing Technology* 55(1):287–290.
[2] Azushima A, Kopp R, Korhonen A, Yang DY, Micari F, Lahoti GD, et al (2008) Severe plastic deformation (SPD) processes for metals. *CIRP Annals – Manufacturing Technology* 57(2):716–735.
[3] Buffa G, Fratini L, Pasta S, Shivpuri R (2008) On the thermo-mechanical loads and the resultant residual stresses in friction stir processing operations. *CIRP Annals – Manufacturing Technology* 57(1):287–290.
[4] Fratini L, Micari F, Buffa G, Ruisi VF (2010) A new fixture for FSW processes of titanium alloys. *CIRP Annals – Manufacturing Technology* 59(1):271–274.
[5] Sketchley PD, Threadgill PL, Wright IG (2002) Rotary friction welding of an Fe_3Al based ODS alloy. *Materials Science and Engineering A* 329–331: 756–762.
[6] Vairis A, Frost M (1999) On the extrusion stage of linear friction welding of Ti 6Al 4V. *Materials Science and Engineering* A271:477–484.
[7] Bhamji I, Preuss M, Threadgill PL, Addison AC (2011) Solid state joining of metals by linear friction welding: a literature review. *Materials Science and Technology* 27(1):2–12.
[8] Romero J, Attallah MM, Preuss M, Karadge M, Bray SE (2009) Effect of the forging pressure on the microstructure and residual stress development in Ti–6Al–4V linear friction welds. *Acta Materialia* 57:5582–5592.
[9] Mary C, Jahazi M (2008) Multi-scale analysis of IN-718 microstructure evolution during linear friction welding. *Advanced Engineering Materials* 10(6): 573–578.
[10] Bhamji I, Preuss M, Threadgill PL, Moat RJ, Addison AC, Peel MJ (2010) Linear friction welding of AISI 316L stainless steel. *Materials Science and Engineering A – Structural Materials Properties Microstructure and Processing* 528(2):680–690.
[11] Rotundo F, Morri A, Ceschini L (2012) Linear friction welding of a 2024 Al alloy: microstructural, tensile and fatigue properties. *The Minerals Metals & Materials Society (TMS) Light Metals* 493–496.
[12] Fratini L, Buffa G, Campanella D, La Spisa D (2012) Investigations on the linear friction welding process through numerical simulations and experiments. *Materials & Design* 40:285–291.